EXTRACTION OF 3D STRAIGHT LINES USING LIDAR DATA AND AERIAL IMAGES

A. Miraliakbari, M. Hahn, H. Arefi, J. Engels

Dept. of Geomatics, Computer Sciences and mathematics, Stuttgart University of Applied Sciences, Stuttgart, Germany
(miapg110, michael.hahn, hossein.arefi, johannes.engels)@hft-stuttgart.de

Commission IV, WG 9

KEY WORDS: Building, Edge, Extraction, Feature, LIDAR, Reconstruction

ABSTRACT:

Light Detection and Ranging (LIDAR) is a technology used for collecting topographic data. Nowadays there are diverse application areas of LIDAR data that include DTM generation and building extraction. 3D representations of buildings extracted from LIDAR data are often quite inaccurate regarding their location of the building edges. High resolution aerial images have the potential to accurately extract 3D straight lines of the building edges. Thus using aerial images to extract building edges accurately is an option in particular if aerial images are available in addition to LIDAR data. In this paper we present a study on straight line parameter estimation based on the line parameterisation proposed by Schenk (2004). We assume that an aerial triangulation is carried out in advance, hence the exterior orientation parameters of all images are known. The LIDAR data are used to get approximate values of straight line parameters and to simplify the line correspondence problem in the aerial images. The straight lines are extracted from the aerial images and the 3D line parameters are estimated. For extraction of straight lines in the aerial images three techniques are used. Two of them are dealing with semi-automatic straight line extraction and third one focuses on automatic line extraction using the Hough transform. Quality of the results is investigated using different number of images and different number of points measured on the building edges

1. INTRODUCTION

Light Detection and Ranging (LIDAR) is a technology utilized in airborne laser scanning systems for collecting 3D point clouds which implicitly represent topographic data. The LIDAR data is an excellent source for generating digital surface models and digital terrain models. In this processes the irregular point clouds are filtered and often interpolated to a regular grid in which the height is given as a function of the rasterised 2D location.

An important application in which LIDAR and aerial images are used is city modelling. Straight lines, which are in the focus of our research, are important features in this context especially if man-made objects have to be reconstructed.

Schenk (2004) discussed the use of straight lines in aerial triangulation. He introduced a four parameter representation of 3D straight lines, where he utilized azimuth and zenith of the straight line and the intersection of the straight line with the XY plane of a rotated coordinate system.

In related research, Abeyratne (2007) used simulated data for image resection and EOP estimation. He compared methods of six parameter and four parameter representation of straight lines with traditional point based photogrammetry.

A starting point of our research is shown in figure 1. The DSM generated from LIDAR data is overlaid with an orthophoto of the corresponding area. The boundary line of the building roof looks rather fuzzy thus no nice straight line can be recognised. This is mainly an impact of the interpolation in the LIDAR data thus it is to be expected that the roof boundary can not be extracted very accurately from the LIDAR data.

Lines in the high resolution aerial images do not have this kind of deficit thus it would be near at hand to use images for extracting 3D lines. But extracting 3D straight lines from overlapping aerial images is much more complicated than extracting 3D lines directly from the LIDAR data.

Figure 1. Magnified area of superimposing the LIDAR data with ortho photo

If both kinds of data are available the simultaneous use of LIDAR and image data will reduce the complexity 3D line reconstruction. This can be considered as an approach to improve the accuracy of LIDAR based 3D line reconstruction by using the aerial images.

In the following we give some more theoretical background, point out our methodology, discuss the achieved results and draw some conclusions.

2. THEORETICAL BACKGROUND

Points are the basic elements in most algorithms of photogrammetry. Influenced by developments in computer vision however there has been efforts to develop feature based method also.

Schenk argued that lines can be taken as an alternative to points in photogrammetry, because "1. A typical area of scenes contains more linear features than well defined points. 2. Establishing correspondences between [linear] features in different images and /or images and object space is more reliable than point matching" (Schenk, 2004).

2.1 Line representation

To solve fundamental tasks of orientation with straight lines, optimal line representations in 3D Euclidean space should meet the following requirements:

- The number of parameters should be equal to the degree of freedom of a 3D line.
- Representation should be unique and free of singularities.

Parametric representation of manifolds in object space allows the specification of any point on the feature. A four parameter representation of the line is uniquely given by the 4- tuple (Φ, θ, x_0, y_0).
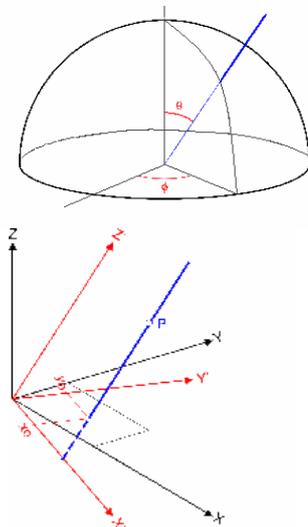

Figure 2. Illustration of the concept of 4-parameter representation (adapted from Schenk, 2004)

Φ is the azimuth and θ is the zenith angle of the straight line. A new coordinate system is defined in such a way that the new **Z** axis is parallel to direction of the straight line. The position of the line is defined by the point (x_0, y_0) where the X-Y plane in rotated coordinate system is intersecting the line. All the points on the straight line have a value namely s_i as a point position parameter along the line. Thus the distance between the s_i and s_{i+1} is calculated as $s_{i+1} - s_i$ (the unit is in meter) (Schenk, 2004).

2.2 Mapping between point representation and parametric representation of 3D straight line

To find the rotation matrix between the original (initial) coordinate system and the line oriented coordinate system, the following expression is applied. As a first step, there should be a conversion of coordinates from Cartesian (X, Y, Z) to the spherical coordinate (Φ, θ, ρ). ρ is not applied in this task because the procedure doesn't deal with the radius. The rotation matrix which is necessary for this conversion is $R_{\Phi\theta}$:

$$R_{\phi\theta} = R_\theta \cdot R_\phi = \begin{bmatrix} \cos\theta\cos\phi & \cos\theta\sin\phi & -\sin\theta \\ -\sin\phi & \cos\phi & 0 \\ \sin\theta\cos\phi & \sin\theta\sin\phi & \cos\theta \end{bmatrix} \quad (1)$$

A point on the straight line is represented with respect to the new coordinate system according to:

$$P' = R_{\phi\theta} \cdot P = \begin{bmatrix} x_0 \\ y_0 \\ s \end{bmatrix} \quad (2)$$

$$p = R_{\phi\theta}^T \cdot p' = \begin{bmatrix} \cos\theta\cos\phi \cdot x_0 - \sin\phi \cdot y_0 + \sin\theta\cos\phi \cdot s \\ \cos\theta\sin\phi \cdot x_0 + \cos\phi \cdot y_0 + \sin\theta\sin\phi \cdot s \\ -\sin\theta \cdot x_0 + \cos\theta \cdot s \end{bmatrix} = \begin{bmatrix} X \\ Y \\ Z \end{bmatrix} \quad (3)$$

X, Y and Z are object coordinates of the point.

2.3 Combination of collinearity equations and four parameter representation

The parametric representation of the manifold in object space allows the specification of any point on the manifold. The collinearity model looks for the closest point in the manifold to the projection ray. Equation (3) defines a parametric representation of 3D straight lines, and expresses the relationship between an arbitrary point **p** on the 3D line and the four parameter representation (Schenk, 2004). By means of the known EOP derived from aerial triangulation and the four-parameter equation, the collinearity equations can be applied to the running point on the straight line in object space. This is achieved by inserting the parametric representation of the line into the collinearity equations.

$$\begin{bmatrix} U \\ V \\ W \end{bmatrix} = R^T \cdot \left(\begin{bmatrix} \cos\theta\cos\phi \cdot x_0 - \sin\phi \cdot y_0 + \sin\theta\cos\phi \cdot s \\ \cos\theta\sin\phi \cdot x_0 + \cos\phi \cdot y_0 + \sin\theta\sin\phi \cdot s \\ -\sin\theta \cdot x_0 + \cos\theta \cdot s \end{bmatrix} - \begin{bmatrix} X_0 \\ Y_0 \\ Z_0 \end{bmatrix} \right) \quad (4)$$

$$x = -f \cdot \frac{U}{W} \qquad y = -f \cdot \frac{V}{W} \quad (5)$$

Regarding to the equation (3) and general form of collinearity equations (5), there will be five unknowns in the final combined collinearity equations. As the EOP are considered to be known in the study, the unknown parameters are the four parameters of line representation (ϕ, θ, x_0, y_0) and one additional unknown (s) for each point as an element of the straight line.

2.4 Adjustment model to solve unknown parameters

The general form of adjustment which will be used for nonlinear observation equations is represented below (least square adjustment):

$$\delta x = \left(A^T A\right)^{-1} A(l - l_0) \quad (6)$$

In this formula *A* is the design matrix, *l* is observation vector and l_0 approximate values for the observations based on initial values for the unknown parameters.

The residual vector *v* follows from

$$v = A\delta x - (l - l_0) \qquad (7)$$

In this study the straight line parameters have to be estimated and the accuracy of the estimated parameters is important. The covariance matrix of the unknown is computed by multiplication of estimated factor variance ($\hat{\sigma}_0^2$) and the cofactor matrix (N^{-1}).

$$\hat{C}_{\hat{x}\hat{x}} = \hat{\sigma}_0^2 N^{-1} \qquad (8)$$

The diagonal elements of

$$\hat{C}_{\hat{x}\hat{x}} = C_{\theta\varphi x_0 y_0 z} \qquad (9)$$

give the accuracy of all line parameters of interest. In order to have "tangible" results of the unknown's accuracy, it is useful to calculate a point based accuracy using X, Y, Z coordinates in the object coordinate system.

By using variance propagation rule the covariance matrix of X Y Z will be calculated as:

$$C_{xyz} = M C_{\theta\varphi x_0 y_0 s} M^T \quad (10)$$

Where M is Jacobian matrix formulated as follows:

$$M = \begin{bmatrix} \frac{\partial X}{\partial \theta} & \frac{\partial X}{\partial \varphi} & \frac{\partial X}{\partial x_0} & \frac{\partial X}{\partial y_0} & \frac{\partial X}{\partial s} \\ \frac{\partial Y}{\partial \theta} & \frac{\partial Y}{\partial \varphi} & \frac{\partial Y}{\partial x_0} & \frac{\partial Y}{\partial y_0} & \frac{\partial Y}{\partial s} \\ \frac{\partial Z}{\partial \theta} & \frac{\partial Z}{\partial \varphi} & \frac{\partial Z}{\partial x_0} & \frac{\partial Z}{\partial y_0} & \frac{\partial Z}{\partial s} \end{bmatrix} (11)$$

3. METHODOLOGY

The main goal of this study is the estimation of 3D straight line parameters. Those parameters are ϕ, θ, x_o, y_o and s as parameter of point position on the straight line.

This is realised by taking advantage of the LIDAR data in a first step in which initial values of unknown line parameters are calculated and search space for finding corresponding lines in the images is significantly narrowed down. In a second step the high resolution aerial images are used for extraction the corresponding lines and estimating the unknown 3D line parameters.

3.1 Utilizing LIDAR data to calculate initial values of unknown parameters

The main objects used in this study are the buildings, so the last pulse range data are used. The endpoints of the building edges are interactively measured in the LIDAR data (cf. figure 3 as an example). With this measured endpoint coordinates the straight line parameters (ϕ, θ, x_o, y_o, s) are determined.
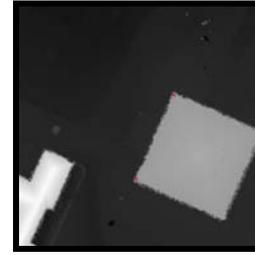

Figure3. Sample of LIDAR range Last Pulse data (endpoints are in red colour)

$(X, Y, Z)_i$ are object coordinates of the endpoints of the building edges. From those the straight line parameters are simply calculated according to

$$\theta = \pi/2 - Arc\tan\left(\frac{\Delta Z}{\sqrt{\Delta X^2 + \Delta Y^2}}\right) \qquad (12)$$

$$\phi = Arc\tan 2\left(\frac{\Delta Y}{\Delta X}\right) \qquad (13)$$

By multiplication of the object point coordinates with the rotation matrix $R_{\phi\theta}$ the line parameters x_0, y_0 and the respective point position parameter s are found:

$$\begin{bmatrix} x_0 \\ y_0 \\ s_1 \end{bmatrix} = R_{\phi\theta} \begin{bmatrix} X_1 \\ Y_1 \\ Z_1 \end{bmatrix} \qquad (14)$$

The calculated straight line parameters from LIDAR data are used as initial values for the next step.

3.2 Using high resolution aerial images for estimating unknown 3D line parameters

There are three different options for straight line measurement/ extraction in/from the images used in the experiments:

1) Measurement of two fixed points (endpoints of the specific straight line).
2) Measurement of sample of the points on the straight line.
3) Selection of endpoints of the straight lines which are automatically extracted.

Figure 4 shows the measured corresponding endpoints of the straight lines in each image. The six unknowns ϕ, θ, x_0, y_0, s_1 and s_2 are estimated from the four observation equations (two points) related to each image. If n is the number of images, the redundancy can be calculated according to r = 4n − 6. Thus with two images there is already a redundancy of two.

Figure 5 illustrates the situation if various points are measured on the straight line without any restriction of the point selection along the line.
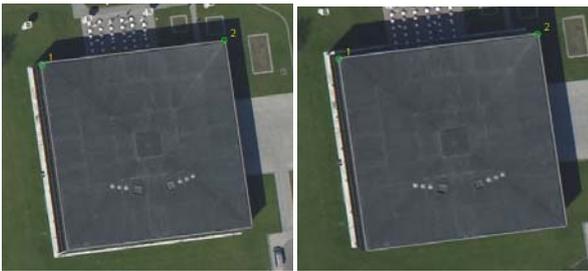
Figure 4. Measurement of endpoints of the building edge of two corresponding images
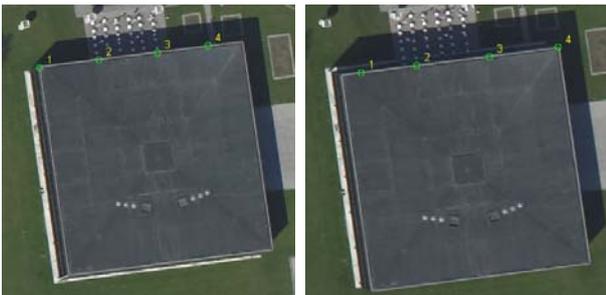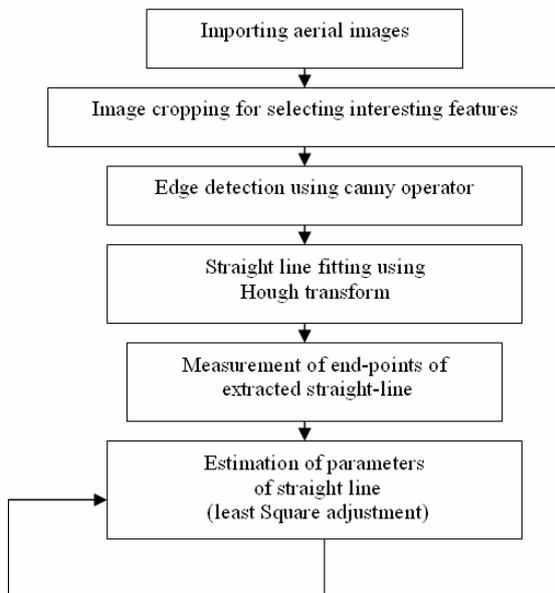

Figure 5. Measurement of multiple points of the building edge in two images

With each measured point in one image, one unknown and two observation equations are added. If **n** is the number of images and **m** is the number of the points measured in each image, the redundancy is r = n m - 4. With two images and two points per image the redundancy is zero.

Slightly more complex is the situation it the straight lines are extracted automatically. The corresponding workflow is shown in Figure 6. The measurement of the endpoint is this case is a tracking process to find the endpoints of the extracted lines.

Figure 6. Flowchart of the third option (automated line extraction)

The developed MATLAB routine uses Canny edge detection and straight line fitting with the Hough transform. The

approximate information given by the interactive line measurement in the LIDAR data defines narrow windows in the images in which the building edges are extracted and approximated by the straight lines. The endpoints of the straight line are found by tracking the points along the line.

The difference of this approach from the other two options is the point selection process. The functional model is the same as for the first option.

4. RESULTS

The test building used in this study is 'Landtag von Baden-Württemberg', the building near the Schlossplatz of Stuttgart in Germany.

Figure 7. Straight lines of the test building

Results for the first option (manual measurement of fixed endpoints) are summarized in Tables 1 and 2 based on the measurement of endpoints in two aerial images only.

Parameters Line No.		θ (rad)	φ (rad)	x_0 (m)	y_0 (m)	s_1 (m)	s_2 (m)
1	I	1.581	1.14	-329.62	-2794.79	2183.8	2235.42
	F	1.568	1.15	-301.25	-2798.62	2179.16	2233.06
2	I	1.558	-0.44	-269.99	2290.11	2756.35	2808.74
	F	1.579	-0.423	-330.97	2242.91	2787.37	2841.51
3	I	1.555	-1.979	-338.18	2877.06	-2194	-2143.01
	F	1.571	-1.993	-304.56	2846.33	-2240.44	-2186.67
4	I	1.570	2.708	-306.97	-2217.38	-2822.99	-2770.45
	F	1.569	2.72	-309.09	-2179.95	-2851.03	-2797.2

Table 1. Comparison of initial (I) parameters and final adjusted (F) parameters of straight lines using four images

Accuracy(m) Line No.	X_1	Y_1	Z_1	X_2	Y_2	Z_2
1	0.14	0.28	0.89	0.15	0.23	0.89
2	0.35	1.58	1.45	0.39	1.22	1.45
3	0.44	0.42	1.65	0.42	0.47	1.65
4	0.4	0.43	1.57	0.37	0.39	1.57

Table 2. Accuracy of endpoints in each adjusted straight line

The average horizontal accuracy is in the order of three to five pixels (20 cm pixel size), the height accuracy of 1 to 1.5 meters is approximately 50% worse. The low redundancy obviously leads to a moderate overall accuracy.

The second option leads to more observation equations and more unknowns, because in this approach the selected points

are selected individually in each image. Therefore the number of s_i values will be bigger.

By using the same example (Figure 7) used already in the first option a quite unsatisfying result is obtained shown in Figure 8.
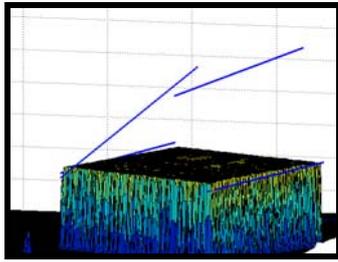

Figure 8. Side view of straight lines extracted by second option

From the estimated accuracy the low quality could be already expected as can be seen in Table 3.

Accuracy(m) Line No.	X_1	Y_1	Z_1	X_2	Y_2	Z_2
1	0.06	0.10	0.46	0.09	0.21	0.47
2	0.01	10.63	0.44	0.12	11.46	0.64
3	0.19	0.29	3.56	3.90	0.96	1.28
4	0.18	3.56	0.96	0.29	3.9	1.26

Table 3. Accuracy of endpoints in each adjusted straight line in second approach

The reason for this low quality was found by investigating the geometry of the 3D lines and the 3D projection centers. Building edges which are nearly parallel to the base (the 3D connecting line of the projection centers) define one plane in the three dimensional object space. The consequence is a de facto singularity in the adjustment of the 3D line parameters.

This singularity can be avoided by using images in which line through the projection centers is perpendicular to the direction of straight lines. So for the lines number 1 and 3, one set of images are used and for the lines number 2 and 4, another set of images are used. The table below shows the accuracy of the endpoints after using appropriate images.

Accuracy(m) Line No.	X_1	Y_1	Z_1	X_2	Y_2	Z_2
1	0.19	0.42	0.98	0.44	0.22	1.24
2	0.09	0.56	0.3	0.68	0.53	0.29
3	0.19	0.42	0.98	0.44	0.22	1.24
4	0.14	0.32	0.5	0.11	0.37	0.46

Table 4. Accuracy of endpoints in each adjusted straight line with appropriate images

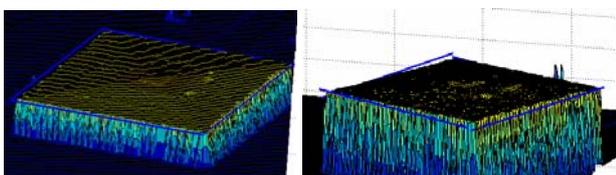The improvement (compared with Figure 8) can be easily seen from the figure below.

Figure 9. Result found by properly selected image pairs. For details see the text.

The approach in which the lines and the endpoints of the lines are automatically selected (option 3) is illustrated in Figures 10 to 12. The test region shows a part of the New Castle in Stuttgart, Germany. One of the extracted edges is shown in Figure 10. End points are found by tracking along the edge.

Figure 10. Straight line extracted by the Hough transform

In a first view the extracted line looks almost perfect. A closer look reveals (Figure 11) that the position of the corresponding endpoints in both aerial images differs by several pixels. These different positions directly influence the result of the adjustment procedure.
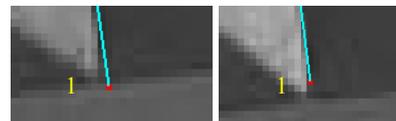

Figure 11. Localised corresponding endpoints in two images
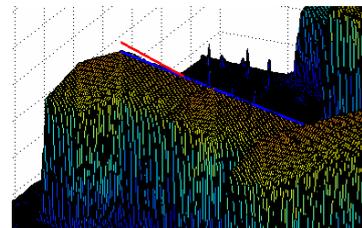

Figure 12. Adjusted straight line (red line) using the endpoints found through the Hough transform and line tracking.

The blue line shows the position of the straight line based on given LIDAR data (initial values). The red line represents position of the extracted straight line which is obviously not fitting to the building ridge perfectly.

5. CONCLUSION

The investigations into 3D line extraction shows that there is still a lot of research required if the goal is to extract 3D lines reliably and accurate. Best results we have got by measuring the endpoints of straight lines manually but this, of course, is not really an alternative to traditional photogrammetric point based restitution.

The automated process with Canny edge detection and Hough line extraction yields results which are even weaker than the results using manual endpoint measurements. Probably the model with four line parameters plus one parameter for each point on the line is not really suited in combination with automated edge feature point extraction.

We started already to formulate the 2D image line and 3D object line parameterisation without any point related parameter. The automated process is currently under investigation and result will be presented in near future. .

REFERENCES

Abeyratne**,** P., Hahn, M. (2007), *An Investigation Into Image Orientation Using Linear Features*, Joint workshop on "Visualization and Exploration of Geospatial Data", Stuttgart, Gemany.

Schenk, T., (2004), *From point based to feature based aerial triangulation.* Photogrammetry and Remote Sensing, Vol. 58, No 5-6, pp. 315-329.

Wolf, P., Ghilani,C., (1997), *Adjustment computation: Statistics and least square in surveying and GIS,* New York.